Aspects of three-dimensional magnetic reconnection

D. Borgogno[1], F. Califano[2], D. Farina[3], D. Grasso[1], F. Pegoraro[2], F. Porcelli[1]
[1] Istituto Nazionale Fisica della Materia and Politecnico di Torino, Italy
[2] Istituto Nazionale Fisica della Materia, Dip. Fisica, Università di Pisa, Italy

1 Introduction

Magnetic reconnection in collisionless regimes is a relevant process in magnetically confined plasmas, both in space and in nowdays tokamak experiments. For reconnection processes that are nearly two-dimensional, 3D effects are of interest, in that they introduce regions of magnetic field line stochasticity centered around the separatrices of 2D magnetic islands where current and vorticity layers are localized. Thus, 3D effects can be expected to alter significantly the spatial structure of these layers and hence the rate at which reconnection can proceed. We present here three main results: (1) the discussion of oblique modes; (2) the characterization of magnetic stochasticity that is produced self-consistently; (3) a measure of the reconnected flux applicable to 3D case.

2 Model equations

We consider here the dissipationless model given in Ref. [1], which describes drift-Alfven perturbations in a plasma immersed in a strong uniform, externally imposed magnetic field, where spatial variations along the field lines are assumed to be small compared to perpendicular variations. In the limit of small ion gyroradii, this system consists of two fluid, quasi neutral electron and ion equations where small scales effects related to the electron temperature, $\rho_s = (T_e/T_i)^{1/2}\varrho_i$, and to electron inertia, $d_e = c/\omega_{pe}$, are retained, but magnetic curvature effects are neglected. We adopt here the notation of Ref. [2]. The equations, normalized to the Alfven time, $\tau = \sqrt{4\pi n m_i}L_x/B_{y0}$, with B_y0 the characteristic magnitude of the equilibrium magnetic field, and to the macroscopic scale length, L, are:

$$\frac{\partial G_\pm}{\partial t} + [\varphi_\pm, G_\pm] = \frac{\partial \varphi_\pm \mp \frac{\varrho_s}{d_e} G_\pm}{\partial z} \tag{1}$$

where $G_\pm = \psi - d_e^2\nabla^2\psi \pm d_e\varrho_s\nabla^2\varphi$, $\varphi_\pm = \varphi \pm (\varrho_s/d_e)\psi$, ψ is the magnetic flux and φ is the stream function. The Poisson brackets are defined as $[A, B] = \mathbf{e}_z \cdot \nabla_\perp A \times \nabla_\perp B$.

3 Results

To solve the system (1) we produced an initial value parallel numerical code based on a finite volumes scheme, where the mean values of the $G_\pm$ fields are advanced in time using an explicit third order Adams-Bashfort scheme. We performed our simulations in a 3D periodic slab geometry, starting from a static equilibrium configuration characterized by the following magnetic field,

$$\vec{B}_{eq} = B_0\vec{e}_z + \nabla\psi_{eq} \times \vec{e}_z, \tag{2}$$

where $\psi_{eq} = \alpha cos(x)$ and $B_0 = -1$. All the runs we show in this paper have been carried out in the so called large Δ' regime, with $\varrho_s = d_e = 0.24$. The integration domain is defined by $-L_x < x < L_x$, $-L_y < y < L_y$ and $-L_z < z < L_z$, with $L_x = \pi$, $L_y = 2\pi$ and $L_z = 16\pi$.

Oblique modes. In the first case we present, we have initialized the code modifying the equilibrium (2), with $\alpha = 0.48$, by an unstable single helicity perturbation, chosen as $\tilde{\psi}(x, y, z, t) = \hat{\psi}(x)exp(ik_y y + ik_z z)$, where $k_y = \pi m/L_y$, $k_z = \pi n/L_z$ and $m = 1$, $n = 1$. Even though the perturbation depends on all three spatial coordinates, it is equivalent to a 2D non symmetric mode, the asymmetry being related to the fact that this mode has a

mixed parity around the corresponding resonant magnetic surface. Actually, after a rotation by a small angle k_z/k_y in the (y,z) plane, the Eqs.(1) can be written as

$$\frac{\partial G_{\pm *}}{\partial t} + [\varphi_{\pm *}, G_{\pm *}] = 0 \tag{3}$$

where $G_{\pm *} = G_{\pm} + (k_z/k_y)x$ and $\varphi_{\pm *} = \varphi_{\pm} + (k_z/k_y)x$. As a consequence of this asymmetry, the magnetic island X-point, where $\nabla\psi_* = \nabla[\psi + (k_z/k_y)x] = 0$, is no longer a stagnation point for the velocity field and therefore it acquires a drift along the direction of the x-axis. This shift becomes appreciable in the nonlinear phase, when the X-point falls very near to the drifting neutral line of $G_{\pm *}$. Since $G_{\pm *}$ are advected with the velocity field $v_{\pm *} = \mathbf{e}_z \times \nabla\varphi_{\pm *}$, at the X-point we find that $v_{x\pm *}$ coincides with the fluid velocity defined by $v_x = -\partial\varphi/\partial y$. This observed drift of the X-point is shown in Fig. (1), where the asterisks represent the numerically evaluated positions of the X-point during the evolution of the instability. The solid line represents the displacement of the X-point, $\delta_X = v_X dt$, calculated using the fluid velocity. During the nonlinear evolution, modes with different helicities are observed, but never seem to reach an appreciable amplitude.

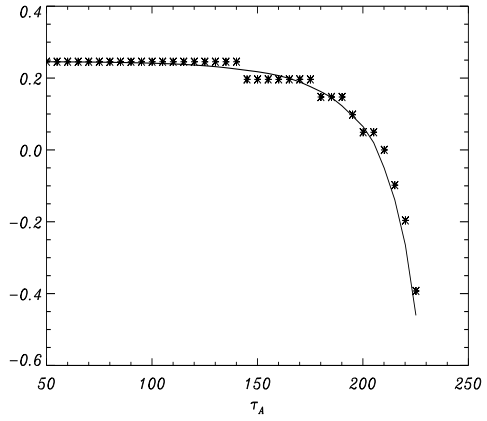

FIG. 1. Comparison between the numerical estimated X-point positions ($*$) and the displacement calculated by the fluid velocity (solid line), during the evolution of an oblique mode.

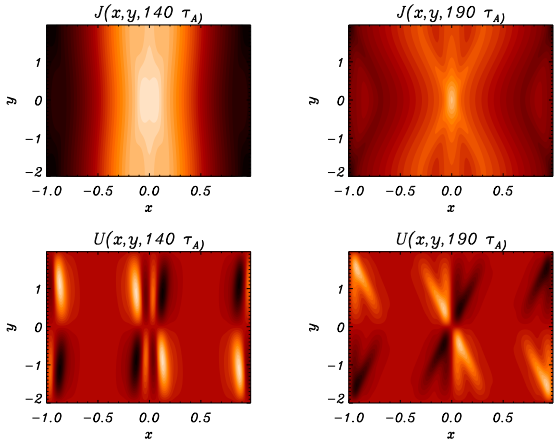

FIG. 2. 2D representation on the $z = -L_z$ section of the topological modification of the current (J) and vorticity (U) layers during the nonlinear evolution for a double helicity perturbation.

Self-consistent magnetic stochasticity. In the second case we present, we turn to the truly 3D problem, where several helicities are present in the initial perturbation. In general, we start with two initial unstable perturbations, such as $\hat{\psi}_1(x)exp(ik_{y1}y + ik_{z1}z)$ and $\hat{\psi}_2 exp(ik_{y2}y + ik_{z2}z)$, and we observe the growth of several additional helicities due to the non linear coupling. In all our simulations, performed with different pairs of wave numbers (k_y, k_z) and starting amplitudes $\hat{\psi}$, we identify a quasilinear phase, during which these higher order modes grow in agreement with the rates of their parent perturbations. The strong coupling of modes with different helicities is responsible for the change of the current density and vorticity layers structure during the nonlinear evolution. In Fig. (2), we plot the 2D contours of the current density and vorticity on the $z = -L_z$ section at two different times. This case refers to an equilibrium configuration with $\alpha = 0.48$ and an initial perturbation characterized by $k_{y1} = k_{y2} = 1/2$, $k_{z1} = -k_{z2} = 1/16$ and $\hat{\psi}_1 = \hat{\psi}_2$. We see that in the early nonlinear phase (left frames) the two current and vorticity layers, related to the initial perturbations, are still present. At later time (right frames) the two layers merge because of the X-point drift dicussed in the previous section, possibly combined with the mutual attraction

of neighbouring current channels. We point out that, due to the different spatial orientation of the layers, this interaction is different on the various $z = const$ planes.

In the generic 3D case the magnetic field line Hamiltonian, $\psi(x, y, z; t)$, is not integrable, since it describes a dynamical system with $1 + 1/2$ degrees of freedom. Magnetic field lines satisfy the Hamilton equations, where x and y play the role of conjugate variables, z the role of time and the true time t is a parameter. Numerical integration of these equations allows us to produce Poincaré maps for the magnetic field lines. Fig. (3) shows maps at different times for the section $z = 0$. The Hamiltonian $\psi(x, y, z; t)$ is an output of our fluid code, initialized with a perturbation with $k_{y1} = k_{y2} = 1/2$, $k_{z1} = 0$, $k_{z2} = 1/16$, $\hat{\psi}_1 = 0.1\hat{\psi}_2$ and an equilibrium amplitude $\alpha = 0.19$.

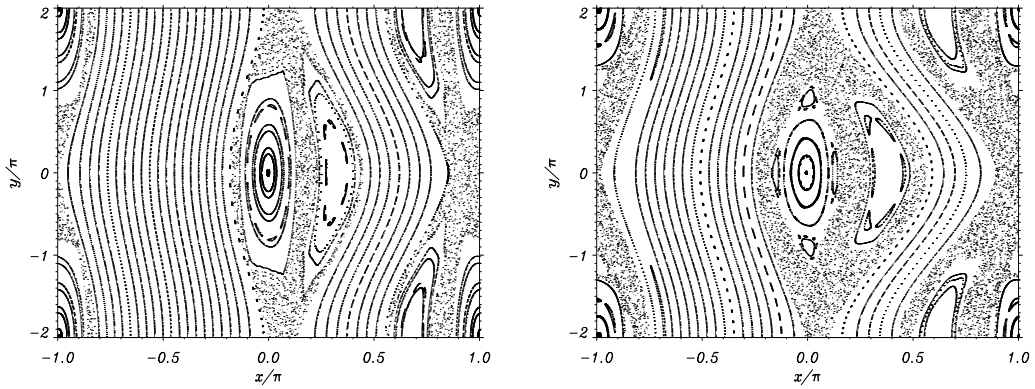

FIG. 3 Poincaré plots of the magnetic field lines on the $z = 0$ section at different times.

It is evident that for large size perturbations few magnetic surfaces survive. Most field lines fill stochastic volumes which in the Poincaré section appear as nearly uniform splatter of dots. The transition to the global stochasticity is in qualitative agreement with the so called "overlap criterion" formulated by Chirikov Ref. [3]. The degree of stochasticity is characterized by a Lyapunov coefficient, which gives the mean exponential rate of the divergence of neighbour trajectories. In our simulations we observe that, at the highest values of the perturbation amplitudes, the average value of the maximum Lyapunov coefficient, normalized to the length L_z, is of the order 1. This means that the typical radial excursion of a magnetic field line in the stochastic region after one toroidal revolution is comparable with the width of the chaotic area itself. Such a high degree of stochasticity can be expected to produce a flattening of the current density in the stochastic regions, when a saturated state is reached. We point out that, since we adopt a periodic equilibrium, resonant magnetic perturbations with equal helicity from adjacent periodicity cells tend to interact strongly. This forces us to stop the simulations before saturation of the magnetic field can occur. Fig. (4) shows the contour plots and the profiles of the current density field on the (x, y) plane, corresponding to the Poincaré maps of Fig. (3). Comparing the profiles with the Poincaré maps we see that a significant variation of the current density in the stochastic regions is still present. This means that at this stage of the process, far away from saturation, no flattening is found.

3D reconnected flux. The standard 2D definition of the reconnected flux and of the reconnection rate, the value of the helical flux at the X-point, can not be easily extended into the 3D case. This difficulty is related with the non integrability of the magnetic field line Hamiltonian in the presence of multiple helicity modes. We propose a new measure of the reconnected flux and of the reconnection rate suitable for 3D configurations in the presence of a constant magnetic guide field. This measure is defined as the total area, A_{tot}, of the stochastic regions and of the enclosed reconnected flux surfaces that are found on a $z = const$ Poincaré map. In the case of a single helicity mode, this definition reduces to the

area of the corresponding magnetic island. This area is in one-to-one correspondence with the reconnected poloidal flux. In Fig. (5), we present a logarithmic plot of the reconnected area for two cases. The time scale has been normalized in terms of the linear growth rate, which corresponds approximately to the linear rate of the highest amplitude initial mode. According with the present definition, we can distinguish three main phases. After an initial linear phase, where the starting modes grow indipendently from each other, we observe a superexponential phase. When the transition to global stochasticity occurs (at $\gamma_{lin}t = 2.5$, in Fig. (5)) the reconnected area starts to grow with a lower rate. We point out that the growth of the reconnected area exhibits very similar features for different helicity combinations. This suggest that, even in this complex 3D setting, the characteristic growth time of the collisionless reconnection process in the nonlinear regime (i.e., before the saturated phase is approched) is of the order of the exponential growth time found in the small-amplitude linear phase.

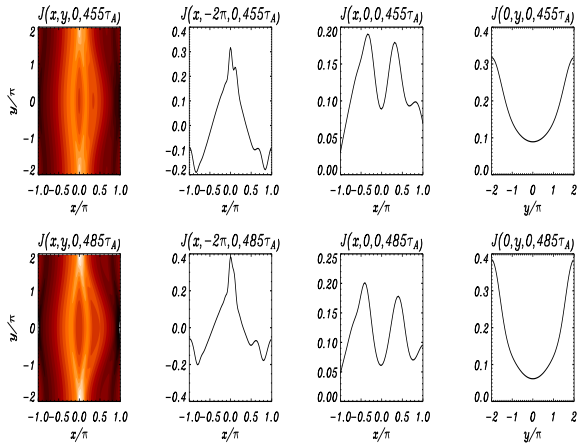

FIG. 4. Contour plots and profiles of current density at two different times, corresponding to the Poincaré maps in Fig.(3).

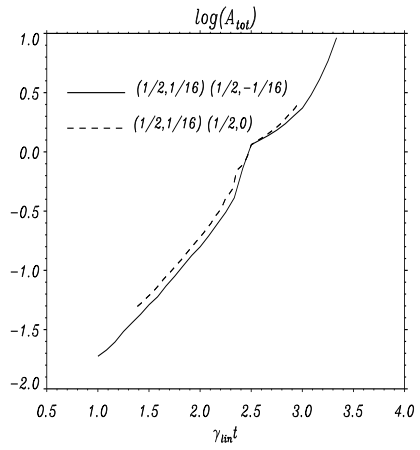

FIG. 5. Reconnected flux for two different cases. Note that the two curves has been shifted in such a way that the transition to the global stochasticity happens at the same instant.

References

[1] T.J. Schep *et al.*, *Phys. Plasmas* **1**, 2843 (1994).

[2] D. Grasso *et al.*, *Phys. Rev. Lett.* **86**, 5051 (2001).

[3] B. V. Chirikov *et al.*, *Phys. Reports* **52**, 265 (1979).